Original article
DOI: https://doi.org/10.18721/JPM.15105

ABNORMAL PARTICLE HEATING IN THE PLASMA DUST STRUCTURES

S. I. Mol'kov✉, *A. S. Shtykov*

Petrozavodsk State University, Petrozavodsk, Russia

✉ tandem@onego.ru

Abstract: In order to explain the nature of abnormal particle heating in the plasma dust structures (PDS) based on helium-group gases, kinetic characteristics of PDS have been studied experimentally and theoretically. To inject the dust component, a container with particles of dispersed materials of different nature was used. The visualization and monitoring of PDS behavior as well as measuring of plasma parameters were carried out via specially designed hardware and software complex. The rates and temperatures of dust particles depending on the discharge conditions were determined experimentally. An analysis of the obtained results made it possible to reveal the process peculiarities and to put forward the explanation of mechanism of heating and dissipation of particle energy in the ordered and chaotic PDSs.

Keywords: plasma dust structure, abnormal particle heating, free-molecular condition, RMS-bias

Citation: Mol'kov S. I., Shtykov A. S., Abnormal particle heating in the plasma dust structures, St. Petersburg Polytechnical State University Journal. Physics and Mathematics. 15 (1) (2022) 52–61. DOI: https://doi.org/10.18721/JPM.15105

Научная статья
УДК 533.9.01
DOI: https://doi.org/10.18721/JPM.15105

АНОМАЛЬНЫЙ РАЗОГРЕВ ЧАСТИЦ В ПЛАЗМЕННО-ПЫЛЕВЫХ СТРУКТУРАХ

С. И. Мольков ✉, *А. С. Штыков*

Петрозаводский государственный университет, г. Петрозаводск, Россия

✉ tandem@onego.ru

Аннотация. С целью объяснения природы аномального разогрева пылевых частиц в плазменно-пылевых структурах (ППС) на основе инертных газов, в работе исследуются экспериментально и теоретически кинетические характеристики ППС. Для инжектирования пылевого компонента применялся контейнер с частицами полидисперсных материалов разной природы (оксид алюминия и цинк). Визуализация и мониторинг поведения ППС, а также измерение параметров плазмы осуществлялись с помощью специально созданного программно-аппаратного комплекса. Экспериментально определены скорости и температуры различных пылевых частиц в зависимости от условий разряда. Анализ полученных результатов позволил выявить особенности процессов и предложить объяснение механизма разогрева и диссипации энергии частиц в упорядоченной и хаотической ППС.

Ключевые слова: плазменно-пылевая структура, аномальный разогрев, свободномолекулярный режим, среднеквадратичное смещение

Для цитирования: Мольков С. И., Штыков А. С. Аномальный разогрев частиц в плазменно-пылевых структурах // Научно-технические ведомости СПбГПУ. Физико-математические науки. 2022. Т. 15. № 1. С. 52–61. DOI: https://doi.org/10.18721/ JPM.15105

Introduction

Dusty plasma is an example of an open non-equilibrium system where a self-assembly process occurs, with dissipative structures emerging [1]. Massive dust particles in weakly ionized plasma effectively dissipate their kinetic energy due to collisions with neutral atoms at a rate ν_{da}, so they are assumed to be in equilibrium with the atomic component and their temperature T_d is equal to the atom temperature T_a ($T_a = 300$ K = 0.026 eV). The mean particle velocity v_d reaches about 0.5 mm/s at a mass $m \approx 0.1$ µg in real experiments. At the same time, the kinetic energy of the dust component particle is about 10 aJ (10^{-17}J), which corresponds to a temperature of the order of 10^3 T_a. The mechanisms behind abnormal heating of the dust component have been linked to stochastic fluctuations in the particle charge [2, 3]. Estimates of T_d values obtained by the formulas given in monograph [4] do not correspond to our experimental data (see the results below), so the true nature of dust particle heating in plasma-dust structures (PDS) is yet to be established definitively.

The goal of this study consisted in describing the behavior of plasma-dust structures, proposing an explanation for the nature of abnormal heating of dust particles in such structures.

Experimental

A plasma crystal setup, described in our earlier study [5], was used for the experiment. A glass discharge tube with a radius of 1.5 cm where the glow discharge plasma was induced and the PDS was generated was filled with the working gas (helium, neon or argon) under a pressure of 0.15 to 3.0 Torr and at a discharge current of 0.1–3.0 mA. A container with particles of different polydisperse materials was used to inject the dust component:

aluminum oxide Al_2O_3 with mean radius $a \approx 23$ µm and mass $m \approx 0.20$ µg;
polydisperse zinc Zn with mean radius $a \approx 28$ µm and $m \approx 0.65$ µg;
same material (Zn), but with $a \approx 8$ µm and $m \approx 0.015$ µg.

The dust structure was visualized with a DTL-316 pulsed semiconductor laser (working wavelength $\lambda = 532$ nm) and a set of lenses producing a laser sheet; the PDS can be observed in the light scattered by this sheet.

The hardware and software system for video images included a Hispec 1 high-speed video camera and the Hispec Control software; the system provided real-time recording for 1 min at different speeds (from 25 to 1500 fps). The experimental setup was assembled so that the electrical characteristics of plasma and the pressure of the plasma-forming gas could be monitored simultaneously. The plasma parameters (electron temperature, charge carrier density) were measured by an automated system for recording the probe characteristics.

Fig. 1 shows the trajectories of zinc particles for discharge in neon under a pressure $p = 1$ Torr, at a discharge current $I = 1.5$ mA and at different camera speeds.

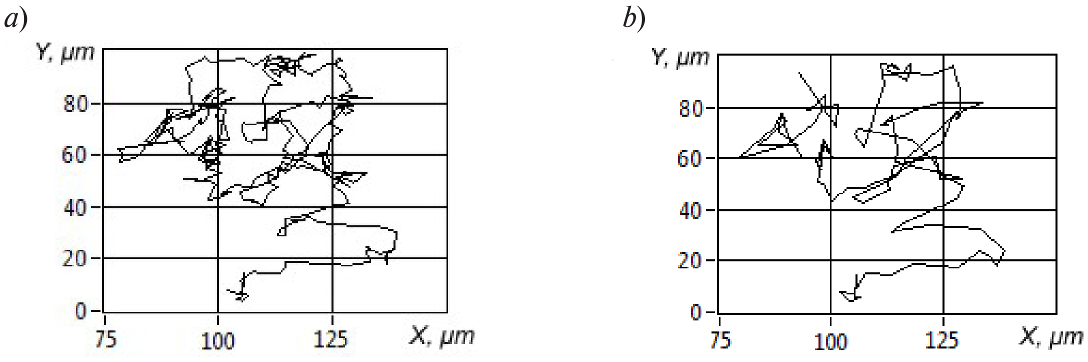

Fig. 1. Trajectories of zinc dust particles in neon,
obtained at two camera speeds, fps: 1500 (*a*) and 250 (*b*);
pressure $p = 1$ Torr, discharge current $I = 1.5$ mA

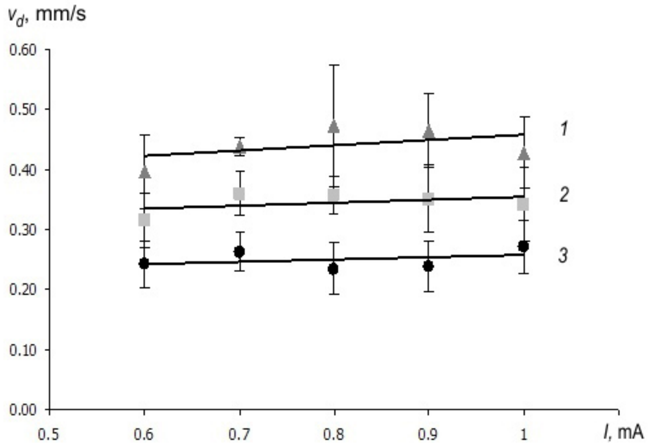

Fig. 2. Experimental dependences of mean velocity on the discharge current for Al_2O_3 particles in neon at various neon pressures p, Torr: 0.3 (*1*), 0.6 (*2*) and 0.9 (*3*)

Particle velocity is determined by the ratio of the distance between two positions of the particle to the time interval equal to the inverse frame rate n of video recording. The error in determining the velocity first decreases with increasing frame rate n, and then starts to increase as the distance traveled by the particle between the frames becomes comparable to its size. The optimal range of the high-speed camera's frame rates was determined experimentally and amounted to 250–500 fps [5]; this was based on the results of particle velocity measurements for PDS in the 'liquid' phase including particles levitating in argon, neon or helium plasma. The confidence interval for the mean velocity v_d, determined through a series of measurements, amounted to 90%.

Fig. 2 shows the typical dependences of the mean velocity on the discharge current for aluminum oxide particles in neon at different pressures.

Analysis of the experimental data obtained for the mean particle velocity v_d and the velocity-related temperature $T_d = m_d v_d^2/3k$ (k is the Boltzmann constant) shows that they weakly depend on current and are governed by pressure. In addition to the particle velocity measurements, experiments were conducted to find the distances r_d between the particles depending on the discharge conditions. The following approximate formulas hold true in the given range of discharge conditions:

$$v_d \approx v_0\sqrt{\frac{p_0}{p}},\ T_d \approx T_0\frac{p_0}{p} = \frac{m_d v_0^2}{3k}\frac{p_0}{p},\ r_d \approx r_0\left(1+\mu I\right)\sqrt{\frac{p}{p_0}}, \qquad (1)$$

where v_0, mm/s, is the velocity at $p = p_0 = 0.3$ Torr; T_0, K, is the corresponding temperature; I, mA, is the current.

The quantities v_0, r_0 and the constant μ depend on the type of gas and the characteristics of the particles. For example, they take the following values for PDS in Ne–Al_2O_3:

$$v_0 = 0.44 \text{ mm/s},\ T_0 = 9.4 \cdot 10^5 \text{ K},\ r_0 = 130\ \mu\text{m},\ \mu = 0.38.$$

The pressure determines the effective electron temperature T_e, and the discharge current determines the electron density n_0. The lighter the plasma-forming gas, the smaller the value of r_d. For example, the following dependence is observed for $p = 0.6$ Torr:

Gas	r_d, μm
Ar	330
Ne	200
He	140

This may be due to the difference in electron temperatures T_e at the same pressures and currents. In particular, the following relationship is observed at $I = 1$ mA, $pR = 0.9$ Torr·cm (R, cm, is the tube radius):

Gas	T_e, eV
Ar	1.4
Ne	2.8
He	3.7

Indeed, according to Eq. (10) (see below), the charge ratio $|Z_d|$ for particles of the same size for different Ar : Ne : He gases is defined as 1.0 : 2.0 : 2.6, which correlates well with the ratio for the inverse distances $(r_d)^{-1}$ between the particles: 1.0 : 1.7 : 2.3.

The distribution of velocity projections along the horizontal axis (Ox) and along the vertical axis (Oy), determined both for an individual dust particle and for their ensemble, corresponds to a normal distribution, which is consistent with the results obtained in [6].

Determination of dust particle velocity and temperature

The distribution function (DF) along the components of dust particle velocity is approximated by a Maxwellian DF [7]:

$$f(\nu_i) = \sqrt{\frac{\beta}{\pi}} \exp\{-\beta \nu_i^2\}, \tag{2}$$

where $\beta = m_d/2kT_{di}$; T_{di} are the temperatures of dust particles in the vertical ($i = y$) and horizontal ($i = x$) planes; m_d is the mass of dust particles.

Then we obtain the following expression for T_{di} (K):

$$T_{di} = \frac{m_d}{(2\ln 2)k} \left(\frac{\Delta \nu_i}{2} \right)^2,$$

$$\text{or } T_{di}\,[\text{K}] = 1.3 \cdot 10^{16} m_d \Delta v_i^2, \tag{3}$$

where Δv_i is the DF width at half-maximum; m_d is measured in kg, and Δv_i in mm/s.

We analyze the experimental data, for example, for the discharge in argon with Al_2O_3 dust particles with a mass $m_d = 0.2$ μg, for $p = 0.6$ Torr, $I = 0.6$ mA, obtaining that $\Delta v_x = 0.35$ mm/s, $\Delta v_y = 0.53$ mm/s. Calculation by Eq. (2) gives the temperature values along the axes x and y:

$$T_{dx} \approx 3.2 \cdot 10^5 \text{ K} \approx 27 \text{ eV}; T_{dy} \approx 7.3 \cdot 10^5 \text{ K} \approx 63 \text{ eV}.$$

Thus, the DF of dust particles is anisotropic.

The chaotic velocity of the dust component v_d is related to the temperature of the dust particles as

$$m_d v_d^2 / 2 = 3T_d / 2,$$

where $T_d = (2T_{dx} + T_{dy})/3$.

Then the temperature T_d (K) of the dust particles follows the expression

$$T_d = 2.4 \cdot 10^{16} m_d v_d^2, \tag{4}$$

where m_d is expressed in kg, and v_d in mm/s.

Equation of the energy balance and temperature of the dust particles

To establish the mechanism by which dust particles are heated to temperatures at about a few tens of electron volts and are subsequently cooled, we should consider the equation for particle motion:

$$m_d \frac{d\mathbf{u}}{dt} = eZ_d \mathbf{E} - m_d \nu_{da} \mathbf{u} + \mathbf{f}_r, \tag{5}$$

where eZ_d is the charge of the dust particle; **u** is the instantaneous velocity of the particle; ν_{da} is the rate of momentum transfer for collisions between the particle and the atoms; **E** is the local strength of the electric field; $\mathbf{f}_r$ is a random Langevin force due to collisions with atoms, ions and electrons.

The momentum transfer rate ν_{da} given the Knudsen number $\mathrm{Kn} = \lambda_a/a >> 1$ (λ_a is the mean free path of the atom, a is the particle radius) for free molecular flow is expressed as follows [4]:

$$\nu_{da} = \frac{8\sqrt{2\pi}\gamma}{3}\frac{a^2 n_a T_a}{m_d \nu_{T_a}}, \tag{6}$$

or

$$\nu_{da} = 1.16\cdot 10^{-11} a^2 (p/m_d)(m_a/T_a)^{1/2},$$

where a, m, is the dust particle radius; p, Torr, is the pressure, m_d, kg, is the dust particle mass, m_a, u, is the atomic mass in the plasma-forming gas; $v_{Ta} = \sqrt{T_a/m_a}$ is the thermal velocity of atoms; γ is the accommodation coefficient characterizing the collisions between the atoms and the dust particle, $1 < \gamma < 1.39$ ($\gamma = 1.2$ in the calculation formula).

Multiplying Eq. (5) by **u** and averaging it over an ensemble of dust particles within a unit volume, we obtain:

$$n_d \frac{d}{dt}\frac{m_d\left\langle u^2\right\rangle}{2} = \left\langle \mathbf{j}_d\mathbf{E}\right\rangle - 2\nu_{da} n_d \frac{m_d\left\langle u^2\right\rangle}{2} + n_d\left\langle \mathbf{u}\mathbf{f}_r\right\rangle, \tag{7}$$

where the last term after averaging is substituted by zero (because there is no correlation between $\mathbf{f}_r$ and **u**); $\mathbf{j}_d$ is the current density of dust particles; **E** is the local strength of the electric field near the particle; n_d is the density of dust particles; $\langle \mathbf{j}_d\mathbf{E}\rangle = W_d$ is the power spectral density generated by the discharge and spent on heating dust particles with the averaging condition imposed not only over the ensemble, but also over time, since the quantities $\mathbf{j}_d$ and **E** fluctuate around the average values.

Bearing in mind that $\langle u^2\rangle = \nu_d^2$, as well as the relationship between the temperature and velocity of dust particles, we obtain an equation for the dust particle temperature:

$$\frac{dT_d}{dt} + 2\nu_{da}T_d = \frac{2W_d}{3n_d k}. \tag{8}$$

Solving this equation with the initial condition $T_d = T_a$, we obtain a time dependence (t is the time) for the dust particle temperature:

$$T_d = T_a \exp\left\{-2\nu_{da}t\right\} + \frac{W_d}{3n_d\nu_{da}k}\left(1 - \exp\left\{-2\nu_{da}t\right\}\right). \tag{9}$$

The dust component is heated in a characteristic time $\tau \approx (2\nu_{da})^{-1}$ to the temperature determined by the multiplier $W_d/3n_d\nu_{da}k$. In view of expression (1), the dependence of W_d on pressure takes the form $W_d \sim 1/p^{3/2}$, which approximately corresponds to the experimental data (see Table). The quantity W_d can be estimated from the values of experimentally measured temperatures. In our case, it depends on the pressure and current, amounting to about $W_d \sim 10^{-11}$ W/cm^3, which is significantly less than the power density dissipated in the discharge (10^{-5} W/cm^3). The source of dust particle heating $W_d = \langle \mathbf{j}_d\mathbf{E}\rangle$ is related to their temperature T_d by the ratio $W_d/3n_d\nu_{da}kT_d$. Energy dissipation of dust particles occurs upon braking due to collision with gas atoms.

Table shows the experimental and calculated data we obtained for the Ne–Al_2O_3 PDS under various pressures at the discharge current $I = 0.6$ mA. The given characteristics of the PDS are necessary to substantiate the conclusions formulated. The particle charge, measured in elementary charges, is determined by the balance of ion and electron fluxes in plasma, taking into account the emission processes on the surface [8]:

$$\left|Z_d\right| = \frac{4\pi\varepsilon_0 a}{e^2} T_e \eta_W\left(\tau_e\right) = 694 a T_e \eta_W\left(\tau_e\right), \quad (10)$$

where τ_e is the normalized electron temperature ($\tau_e = T_e/T_a$); η_W is the dimensionless potential of the particle depending on τ_e; the quantity a is expressed in μm, T_e in eV. As the temperature T_e increases, the potential η_W decreases, so that $\eta_W T_e \approx$ const [9].

The value of Z_d, calculated taking into account the uncertainty in the properties of the particle surface (degree of roughness, types of emission), yields $|Z_d| = (3 \pm 0.6)10^4$ (in elementary charge units).

We describe the PDS using the nonideality parameter of the system, equal to the ratio of the electrostatic interaction energy between particles to their kinetic energy, i.e., $\Gamma = (eZ_d)^2/r_d T_d$. If $p = 0.3$ Torr, we obtain a value of $\Gamma \approx 100$; melting of the lower PDS section is observed visually in this case. The critical parameter of nonideality Γ_c, corresponding to the phase equilibrium at $r_d/\lambda_D \approx 1$, equals $\Gamma_c = 106$ [1] (λ_D is the Debye shielding radius). If $\Gamma < \Gamma_c$, the plasma-dust system is a liquid; as the pressure increases, the melting stops, and the magnitude of Γ exceeds Γ_c (see the corresponding row in Table), while the PDS is formed as a crystal (in our case, this is a phase with a body-centered cubic lattice (*bcc*)).

Table

Experimental and calculated characteristics of the Ne–Al_2O_3 plasma-dust structure

Parameter	Value for pressure p, Torr			Calculation formula (or experiment)
	0.3	0.6	0.9	
T_e, eV	3.4	2.8	2.5	Experiment/calculation (see [10])
v_d, mm/s	0.44	0.35	0.25	Experiment
T_d, 10^3 K	940	590	300	$T_d = 3m_d v_d^2/k$
	270	193	155	Calculation (see [4])
r_d, μm	160	225	280	Experiment
n_d, 10^5cm^{-3}	2.44	0.88	0.46	$n_d = 10^{12}/r_d^3$
Γ	≈ 100	≈ 120	≈ 180	$\Gamma = (eZ_d)^2/r_d T_d$ (for estimate)
W_d, 10^{-11} W·cm^{-3}	2.28	1.03	0.41	$W_d = 3n_d \nu_{da} kT_d$
r_c, μm	22.0	17.5	12.5	$r_c = \sqrt{3kT_d/\alpha}$
E_d, W/cm	3.67	2.92	2.09	$E_d = \alpha r_c/e\|Z_d\|$
j_d, 10^{-11} A·cm^{-2}	0.62	0.35	0.196	$j_d = W_d/E_d$
r_c/r_d	0.14	0.08	0.045	Lindemann criterion

Notations: T_e, T_d are the effective electron temperature and dust particle (DP) temperature, respectively; v_d, r_d are the mean DP velocity and the distance between the particles; n_d is the DP density; r_c is the mean-squared displacement of DP from the equilibrium position in a conditional crystal lattice; Γ is the nonideality parameter of the system; W_d is the power density released in the discharge and spent on heating dust particles; E_d is the mean strength of the electric field; j_d is DP current density; m_d, eZ_d are the DP mass and charge; ν_{da} is the rate of DP collisions with neutral atoms; α is the elasticity coefficient; k is the Boltzmann constant.

Note. The discharge current is $I = 0.6$ mA for all data.

Table lists, among other parameters, the values of T_d, which we found by calculation using the formulas given in [4]; they are considerably different from our results (given in the row above). Thus, the power of the DP heating source associated with the fluctuation of particle charge induced by the discrete charging current [4], is clearly insufficient for the observed heating of particles.

Consider the quantity $W_d = \langle \mathbf{j}_d \mathbf{E} \rangle$. The current density of dust particles j_d is induced by elementary currents $eZ_d \nu_d / r_d$ near the sites of the crystal lattice. Averaging within a unit volume, we obtain an estimate of the maximum characteristic density of dust particle current: $j_d^{\max} \sim eZ_d n_d \nu_d$. The minimum field strength corresponding to W_d is equal to $E^{\min}{}_d \sim W_d / j_d^{\max}$.

A more accurate value of the field strength near the lattice site can be estimated using the electrostatic oscillation frequency ω_E. For particles of different materials and sizes in the neon discharge for $\omega_E \sim 1/\sqrt{m_d}$, ~10–80 $\mathrm{s}^{-1,}$ and then the coefficient of elasticity is equal to $\alpha = \omega_E^2 m_d \sim (8 \pm 2) 10^{-8}$ kg/s². The elastic force acting on the particle allows to estimate the field strength by the formula $E_r = \alpha r / e|Z_d|$, where r is the radial coordinate.

The potential φ at the distance r from the particle is determined by the expression:

$$\varphi = -\int E_r dr = \alpha r^2 / 2e|Z_d|.$$

Assuming the thermodynamic equilibrium of the dust component and using the theorem on the uniform distribution of kinetic energy over degrees of freedom, we obtain:

$$e|Z_d|\langle \varphi \rangle = \alpha \langle r^2 \rangle / 2 = 3kT_d / 2,$$

$$r_c = \sqrt{\langle r^2 \rangle} = \sqrt{3kT_d / \alpha}. \tag{11}$$

For example, if $T_d = 9.4 \cdot 10^5$ K, we obtain $r_c = 22$ μm, which corresponds to the observed deviations of particles from the equilibrium position (see Fig. 1). The physical meaning of the quantity r_c becomes clear from expression (11): this is the mean-squared displacement of a particle from the equilibrium position in a conditional crystal lattice. Table gives the values of r_c and the corresponding averaged values of $E_d = \alpha r_c / e|Z_d|$ and $j_d = W_d / E_d$, providing the required value W_d. According to the Lindemann criterion for a melting crystal [4], $r_c / r_d \geq 0.15$, which is close to our results: $r_c / r_d = 0.14$.

Thus, the heating source of dust particles is only partially related to their charge fluctuation induced by discrete charging current [2]. This dust particle in lattice site loses the equilibrium position due to the random collisions with gas atoms and because of the force action of the nearest dust particles in constant Brownian motion. The potential energy upon displacement from the lattice site increases by an average of $\alpha r_c^2 / 2$, which is converted into kinetic energy of directed motion $3kT_d/2$.

Conclusion

We have considered the kinetic characteristics of plasma-dust structures (PDS) both experimentally, using high-speed video recording, and theoretically. We determined the velocities and temperatures of dust particles depending on the discharge conditions. Good agreement between theoretical and experimental results was obtained. We have proposed a scenario for the mechanism behind heating and dissipation of particle energy in ordered and chaotic plasma-dust structures.

REFERENCES

1. **Fortov V. E., Khrapak A. G., Khrapak S. A., et al.,** Dusty plasmas, Physics-Uspekhi. 47 (5) (2004) 447–492.

2. **Morfill G. E., Thomas H.,** Plasma crystal, J. Vacuum Sci. & Technol. A. 14 (2) (1996) 490–495.

3. **Vaulina O. S., Nefedov A. P., Petrov O. F., Khrapak S. A.,** Role of stochastic fluctuations in the charge on macroscopic particles in dusty plasmas, JETP. 88 (6) (1999) 1130–1136.

4. **Vaulina O. S., Petrov O. F., Fortov V. E., et al.,** Pylevaya plazma: eksperiment i teoriya [Dusty plasmas: Experiment and theory], Fizmatlit, Moscow, 2009 (in Russian).

5. **Shtykov A. S.,** The measuring of the kinetic characteristics values of dusty plasma using the high-speed video camera, Proceedings of Petrozavodsk State University. Natural & Engineering Sciences. (6 (151)) (2015) 121–123 (in Russian).

6. **Zharikov N. E., Piskunov A. A., Podryadchikov S. F., et al.,** Dusty structure and microparticle properties modification in complex plasma, Proceedings of Petrozavodsk State University. Natural & Engineering Sciences. (6 (111)) (2010) 99–108 (in Russian).

7. **Biberman, L. M., Vorob'ev V. S., Yakubov I. T.,** Kinetika neravnovesnoy nizkotemperaturnoy plazmy [Kinetics of nonequilibrium low temperature plasma], Nauka, Moscow, 1982 (in Russian).

8. **Mol'kov S. I., Savin V. N.,** Mechanisms of dust grain charging in plasma with allowance for electron emission processes, Plasma Physics Reports. 43 (2) (2017) 202–212.

9. **Savin V. N., Mol'kov S. I.,** The effect of electron emission processes on micro- and nanoparticle charges in the dusty plasma: the accounting for engineering, St. Petersburg State Polytechnical University Journal. Physics and Mathematics. (3(248)) (2016) 78–87 (in Russian).

10. **Prokhorova E. I., Platonov A. A., Molkov S. I., et al.,** The effect of material and roughness of the probe surface on probe characteristics, Plasma Physics Reports. 46 (5) (2020) 521–526.

СПИСОК ЛИТЕРАТУРЫ

1. **Фортов В. Е., Храпак А. Г., Храпак С. А., Молотков В. И., Петров О. Ф.** Пылевая плазма // Успехи физических наук. 2004. Т. 174. № 5. С. 494–544.

2. **Morfill G. E., Thomas H.** Plasma crystal // Journal of Vacuum Science & Technology. A. 1996. Vol. 14. No. 2. Pp. 490–495.

3. **Ваулина О. С., Нефедов А. П., Петров О. Ф., Храпак С. А.** Роль стохастических флуктуаций заряда макрочастиц в пылевой плазме // Журнал экспериментальной и теоретической физики. 1999. Т. 115. № 6. С. 2067–2079.

4. **Ваулина О. С., Петров О. Ф., Фортов В. Е., Храпак А. Г., Храпак С. А.** Пылевая плазма: эксперимент и теория. М.: Физматлит, 2009, 315 с.

5. **Штыков А. С.** Измерение значений кинетических характеристик плазменно-пылевых систем с помощью высокоскоростной видеосъемки // Ученые записки Петрозаводского государственного университета. Серия: Естественные и технические науки. 2015. № 6 (151). С. 121–123.

6. **Жариков Н. Е., Пискунов А. А., Подрядчиков С. Ф., Семенов А. В., Хахаев А. Д., Щербина А. И.** Модификация свойств плазменно-пылевых структур и микрочастиц в комплексной плазме // Ученые записки Петрозаводского государственного университета. Серия: Естественные и технические науки. 2010. № 6 (111). С. 99–108.

7. **Биберман Л. М., Воробьев В. С., Якубов И. Т.** Кинетика неравновесной низкотемпературной плазмы. М.: Наука, 1982, 376 с.

8. **Мольков С. И., Савин В. Н.** Механизмы зарядки пылевых части в плазме с учетом эмиссионных процессов // Физика плазмы. 2017. Т. 43. № 2. С. 193–202.

9. **Савин В. Н., Мольков С. И.** Учет влияния эмиссионных процессов на заряд микро- и наночастиц в пылевой плазме для технологических приложений // Научно-технические ведомости СПбГПУ. Физико-математические науки. 2016. № 3(248) С. 78–87.

10. **Прохорова Е. И., Платонов А. А., Мольков С. И., Игнахин В. С., Назаров А. И.** Влияние материала и степени шероховатости поверхности зонда на зондовые характеристики // Физика плазмы. 2020. Т. 46. № 5. С. 435–440.

THE AUTHORS

MOL'KOV Sergey I.
Petrozavodsk State University
33, Lenin Ave., Petrozavodsk, 185910, Russia
tandem@onego.ru, molkov@petysu.ru
ORCID: 0000-0002-2792-0320

SHTYKOV Aleksey S.
Petrozavodsk State University
33, Lenin Ave., Petrozavodsk, 185910, Russia
shtykoff@petrsu.ru
ORCID: 0000-0003-4693-8881

СВЕДЕНИЯ ОБ АВТОРАХ

МОЛЬКОВ Сергей Иванович – *доктор физико-математических наук, профессор кафедры электроники и электроэнергетики Петрозаводского государственного университета.*
185910, Россия, г. Петрозаводск, пр. Ленина, 33.
tandem@onego.ru, molkov@petysu.ru
ORCID: 0000-0002-2792-0320

ШТЫКОВ Алексей Сергеевич – *старший преподаватель кафедры информационно-измерительных систем и физической электроники Петрозаводского государственного университета.*
185910, Россия, г. Петрозаводск, пр. Ленина, 33.
shtykoff@petrsu.ru
ORCID: 0000-0003-4693-8881

Received 13.12.2021. Approved after reviewing 07.02.2022. Accepted 08.02.2022.
Статья поступила в редакцию 13.12.2021. Одобрена после рецензирования 07.02.2022. Принята 08.02.2022.